JOURNAL OF BACTERIOLOGY, Sept. 2009, p. 5538–5548 Vol. 191, No. 17
0021-9193/09/$08.00+0 doi:10.1128/JB.00174-09

Metabolic Flux Analysis of *Escherichia coli creB* and *arcA* Mutants Reveals Shared Control of Carbon Catabolism under Microaerobic Growth Conditions▽

Pablo I. Nikel,[1,3,4] Jiangfeng Zhu,[2] Ka-Yiu San,[2] Beatriz S. Méndez,[3] and George N. Bennett[1]*

Department of Biochemistry and Cell Biology[1] and Department of Bioengineering,[2] Rice University, Houston, Texas, and Departamento de Química Biológica, Universidad de Buenos Aires,[3] and Instituto de Investigaciones Biotecnológicas, Universidad Nacional de San Martín,[4] Buenos Aires, Argentina

Received 9 February 2009/Accepted 13 June 2009

***Escherichia coli* has several elaborate sensing mechanisms for response to availability of oxygen and other electron acceptors, as well as the carbon source in the surrounding environment. Among them, the CreBC and ArcAB two-component signal transduction systems are responsible for regulation of carbon source utilization and redox control in response to oxygen availability, respectively. We assessed the role of CreBC and ArcAB in regulating the central carbon metabolism of *E. coli* under microaerobic conditions by means of ^{13}C-labeling experiments in chemostat cultures of a wild-type strain, Δ*creB* and Δ*arcA* single mutants, and a Δ*creB* Δ*arcA* double mutant. Continuous cultures were conducted at $D = 0.1\ h^{-1}$ under carbon-limited conditions with restricted oxygen supply. Although all experimental strains metabolized glucose mainly through the Embden-Meyerhof-Parnas pathway, mutant strains had significantly lower fluxes in both the oxidative and the nonoxidative pentose phosphate pathways. Significant differences were also found at the pyruvate branching point. Both pyruvate-formate lyase and the pyruvate dehydrogenase complex contributed to acetyl-coenzyme A synthesis from pyruvate, and their activity seemed to be modulated by both ArcAB and CreBC. Strains carrying the *creB* deletion showed a higher biomass yield on glucose compared to the wild-type strain and its Δ*arcA* derivative, which also correlated with higher fluxes from building blocks to biomass. Glyoxylate shunt and lactate dehydrogenase were active mainly in the Δ*arcA* strain. Finally, it was observed that the tricarboxylic acid cycle reactions operated in a rather cyclic fashion under our experimental conditions, with reduced activity in the mutant strains.**

Transcriptional regulation comprises a complex network of global and specific regulators. Global regulators normally have pleiotropic effects on metabolism, since they control the transcription of several operons that belong to different functional groups. In *Escherichia coli*, seven global regulators (ArcA, Crp, Fis, Fnr, Ihf, Lrp, and NarL) directly modulate expression of about one-half of all genes (41). CreBC and ArcAB are two global sensing and regulation systems in *E. coli* which, along with some other regulatory systems, modulate the expression of genes involved in central metabolism and respiratory pathways allowing rapid adaptive responses to carbon source and oxygen availability in the culture environment.

The *cre* (for *c*arbon *s*ource *r*esponsive) locus comprises *creABCD* and was formerly known as the *phoM* locus (4). Whereas *creA* is a hypothetical open reading frame and *creD*, also known as *cet*, encodes an inner-membrane protein of unknown function, *creB* and *creC* encode a two-component system, i.e., a cytoplasmic regulator and a sensor kinase, respectively. After the discovery of CreBC, genes modulated by this system proved elusive. Based on sequence analysis and using bioinformatic tools Avison et al. (5) were able to define a *cre* tag sequence, to which CreB binds in vitro (8), in order to describe the *cre* regulon. Thus far, the *cre* regulon comprises seven genes activated by CreBC (among them, *ackA*/*pta*, *talA*, and *creD*) and one repressed (*malE*), and it is responsive to the carbon source used and oxygen availability. Indeed, expression of genes modulated by CreBC is activated under fermentative growth conditions using glycolytic carbon sources, as well as under aerobic conditions with low-molecular-weight fermentation products as substrate, such as formate or pyruvate (Pyr) (8). Accordingly, *creB* and *creC* mutants show impaired growth in minimal medium using glycerol, Pyr, or acetate as the carbon substrate (5, 47). Very little is known about this system and the extent of its regulation on central metabolism of *E. coli*.

The Arc (for *a*erobic *r*espiration *c*ontrol) system is a two-component signal transduction system composed of ArcA, the cognate response regulator, and ArcB, the membrane-bound sensor kinase (38). The physiological redox state is sensed by ArcB through the pool of oxidized form of quinone electron carriers (23, 40). Under microaerobic conditions, ArcB undergoes autophosphorylation and the phosphate group is then transferred to ArcA through a phosphorelay process (34). ArcA~P modulates the expression of approximately 135 genes (54). Briefly, it represses the expression of the major dehydrogenase enzymes in the tricarboxylic acid (TCA) cycle and the glyoxylate shunt, e.g., those encoded by the genes *gltA*, *acnAB*, *icdA*, *sucABCD*, *sdhCDAB*, *fumA*, *mdh*, and *aceB* (30, 60). Expression of several other primary dehydrogenases, such as those encoded by the genes *glpD*, *lctPRD*, and *lpdA*, are also repressed (38). On the other hand, the *foc-pfl* genes, which

* Corresponding author. Mailing address: Department of Biochemistry and Cell Biology, Rice University, 6100 Main St., Houston, TX 77251-1892. Phone: (713) 348-4920. Fax: (713) 348-5154. E-mail: gbennett@rice.edu.

▽ Published ahead of print on 26 June 2009.

encode Pyr-formate lyase (Pfl), are activated by ArcA (19). Among respiratory pathways, the expression of *cyoABCDE* genes is repressed by ArcA, whereas the expression of *cydAB* genes is activated (10, 31).

Recent publications show an increasing interest in the *E. coli* CreBC regulation system (5, 8), and the interaction of this system with the more thoroughly studied ArcAB two-component system has been pointed out by Nikel et al. (47). Shared global control of the expression of some genes gives more flexibility for cell regulation and allows *E. coli* to better adapt to environmental and nutritional changes. However, information about how metabolic fluxes are concomitantly modulated by these regulatory systems is not available. Recently, it was shown that the most significant role of both CreBC and ArcAB systems takes place under microaerobic conditions of growth (3, 8, 47, 59). However, the nature and extent of the overlapping control of metabolism by these systems is not well understood, and information on the intracellular flux distribution is lacking. The understanding of the pattern of central metabolic flux control by multiple regulators under stressful conditions, particularly with restricted oxygen supply, is important in both ecological and pathogenic situations. Such restricted conditions of carbon and oxygen supply exist in nature in certain environmental niches and occur widely as transient fluctuations that can elicit a selective response from bacterial cells (26). Similar conditions take place in industrial cultures as a consequence of inadequate mixing within the bioreactors, e.g., in operation at high cell density in the fed-batch mode (36).

Active pathways and flux distribution in central carbon metabolism are critical components of a multidimensional physiological representation of the microorganism (65). Usually, phenotypes of knockout mutants are characterized by quantitative physiological analysis, and conclusions on intracellular metabolism are then based on qualitative interpretations of those results. In order to gain deeper insight into the complex metabolic responses, it is necessary to investigate intracellular metabolite concentrations and fluxes. Intracellular reaction rates are commonly estimated by metabolic flux analysis, which provide a holistic perspective of metabolism (64, 73).

Most previous studies on regulation have investigated the function of global regulators at the transcriptional level. Only recently, the impact of metabolic regulation of ArcAB and Fnr (for *f*umarate and *n*itrate *r*espiration) on fermentative metabolite production patterns was studied under different oxygen levels (59, 76). To understand the global metabolic regulatory functions exerted by CreBC and ArcAB, it would be helpful to look at the overall intracellular flux distribution under microaerobic conditions. Experiments based on ^{13}C labeling followed by metabolic flux analysis are a powerful approach for studying metabolic regulation. In the present study, carefully controlled chemostat experiments were conducted for a wild-type *E. coli* strain and its isogenic Δ*creB*, Δ*arcA*, and Δ*creB* Δ*arcA* derivatives under a well-defined microaerobic condition. Steady-state intracellular fluxes were estimated based on ^{13}C-labeling experiments followed by amino acid detection and quantification by gas chromatography-mass spectrometry (GC-MS). Taken together, our results suggest that both CreBC and ArcAB exert an important influence on central carbon catabolic fluxes in *E. coli* growing under carbon-limited conditions with a restricted oxygen supply.

MATERIALS AND METHODS

Bacterial strains and mutant construction. All *E. coli* strains were derivatives of wild-type K1060, a K-12 strain, and are listed in Table 1, along with the plasmids and primers used in this study. IV1060, a Δ*creB* derivative of K1060, was constructed by the method of allelic replacement described by Datsenko and Wanner (14). Briefly, a kanamycin resistance cassette (FRT-*kan*-FRT) was amplified by PCR from template plasmid pKD4 (which was isolated from *E. coli* DH5α λ_{pir}) with primers Δ*creB*-F and Δ*creB*-R. The purified PCR product was subjected to DpnI digestion and electroporated into *E. coli* K1060 carrying pKD46 (a helper plasmid that expresses the λ-Red functions). Insertion of the FRT-*kan*-FRT cassette into the *creB* locus was confirmed with primers *kan*-F and *kan*-R by colony PCR of Km^r recombinants. One isolate was selected (strain IV1060K) and transformed with plasmid pCP20, encoding the yeast FLP recombinase. Km^s transformants were selected at 42°C, and *kan* gene excision, as well as *creB* deletion, was confirmed with primers *creB*-F and *creB*-R. Construction of strain CT1062 (Δ*arcA*) has been previously described (46). Strain IV1062 (Δ*creB* Δ*arcA*) was constructed by following a similar procedure as for IV1060, but using CT1062 as the host strain. Primers *creB*-F and *creB*-R, as well as *arcA*-F and *arcA*-R, were used in order to confirm the genotype of the double mutant. Phenotypic characterization of the strains was carried out by plating *arcA* strains onto toluidine blue O plates. Since *arcA* mutants are sensitive to redox dyes (53), no growth was observed for strains CT1062, IV1062K, and IV1062 (data not shown). The Cre phenotype was qualitatively checked by impaired growth of strains carrying the *creB* deletion in minimal medium with acetate as the sole carbon source (47).

Medium and chemostat culture conditions. A 2-liter bioreactor (BioFlo 110; New Brunswick Scientific, Edison, NJ) was used for all cultivations, and the working volume was maintained at 1 liter. Glucose-limited chemostat cultures were conducted at a constant dilution rate (D) of 0.10 ± 0.01 h^{-1}, using 20 mM glucose as the sole carbon source. The working volume was kept constant by removal of effluent from the surface of the culture using a peristaltic pump. The medium used was a minimal salt medium containing (per liter of deionized H_2O): 7.0 g of Na_2HPO_4, 3.0 g of KH_2PO_4, 0.5 g of NaCl, 1.0 g of NH_4Cl, 0.2 g of $MgSO_4$, 0.01 g of $CaCl_2$, and 6 mg of thiamine-HCl. $MgSO_4$, $CaCl_2$, and thiamine-HCl were added to the salt medium after autoclaving and cooling as filter-sterilized stock solutions. Foam was suppressed by adding 20 μl of Antifoam B (Sigma-Aldrich, St. Louis, MO) $liter^{-1}$ at the onset of the cultivation. The pH value was controlled at 7.00 ± 0.05 by the automatic addition of 3 M NaOH or 1.5 M H_2SO_4 as required and was double-checked by periodic offline measurements. Temperature was set at 37.0 ± 0.2°C. The bioreactor was purged with a filter-sterilized mixture of 2.5% O_2 in N_2 at a flow rate of 500 ml min^{-1} and maintaining the agitation speed at 285 rpm, similar to the conditions described by Shalel-Levanon et al. (59). Polarographic measurements of residual oxygen concentration in the culture medium confirmed consistent microaerobic conditions among different runs (data not shown). The above-described experimental setup was chosen since it was previously shown that both ArcAB and CreBC systems exert their influence in a more evident fashion under such conditions with restricted oxygen supply (3, 8, 47, 59). Inocula for bioreactor cultures were grown overnight in 250-ml Erlenmeyer flasks at 37°C in a water shaker (250 rpm) from a few picked colonies, using 50 ml of the minimal medium described above.

Labeling experiments. Labeling experiments were started after the cultures reached the steady state. We assumed that the steady state was attained when the optical density at 600 nm remained constant for at least three residence times, and periodic measurements of extracellular metabolites gave consistent results. Unlabeled feeding medium was replaced by an identical salt medium but containing 16 mM unlabeled glucose, 2 mM [U-^{13}C]glucose, and 2 mM [1-^{13}C]glucose (^{13}C content > 99%; Calbiochem, San Diego, CA). Biomass samples were taken after at least another residence time for GC-MS analysis. Cells in 500 ml of culture were harvested by centrifugation for 15 min at 4°C and $10,000 \times g$. Cell pellets were washed three times with cold 20 mM Tris-HCl (pH 7.6) and resuspended in 10 ml of 6 M HCl in sealed Pyrex glass tubes. The mixture was hydrolyzed for 15 h at 105°C, and after cooling at room temperature the resulting hydrolysate was filtered through a 0.22-μm-pore-size filter and evaporated to dryness. Since cysteine and tryptophan were completely oxidized while asparagine and glutamine were deaminated during HCl hydrolysis, there were 16 proteinogenic amino acids in the hydrolysate (66). Dried hydrolysates were partially dissolved in 3 ml of hot acetonitrile, filtered, and stored refrigerated thereafter. For measurements, 150 μl of acetonitrile containing the hydrolysate was combined with 150 μl of derivatization-grade *N*-methyl-*N*-(*tert*-butyldimethylsilyl)trifluoroacetamide (Sigma-Aldrich) in a glass vial. The mixture was incubated for 30 min at 110°C for complete derivatization (15). After cooling to room

TABLE 1. *Escherichia coli* strains, plasmids, and primers used in this study

Strain, plasmid, or primer[a]	Relevant characteristics[b]	Source or reference
E. coli strain		
DH5α λ_{pir}	Strain used for plasmid maintenance; ϕ80*lacZ*ΔM15 *recA1 endA1 gyrA96 thi-1 hsdR17*(r_K^- m_K^+) *supE44 relA1 deoR* Δ(*lacZYA-argF*)*U169*; λ_{pir} lysogen	20
K1060*	K-12 derivative considered wild type in this study; F^- λ^- *fadE62 lacI60 tyrT58*(AS) *fabB5 mel-1*	51
IV1060K	Same as K1060, but Δ*creB*::FRT-*kan*-FRT; Km^r	This study
IV1060	Same as K1060, but Δ*creB*	This study
CT1062	Same as K1060, but Δ*arcA*	46
IV1062K	Same as CT1062, but Δ*creB*::FRT-*kan*-FRT; Km^r	This study
IV1062	Same as CT1062, but Δ*creB*	This study
Plasmid		
pKD46	Vector expressing the Red genes (γ, β, and *exo*) from phage λ under the arabinose-inducible *araB* promoter, *oriR101*, *repA101*(Ts); Ap^r	14
pKD4	Template plasmid for *kan* flanked by FRT sequences, *oriR*γ; Ap^r Km^r	14
pCP20	Helper plasmid, *FLP* λ *c*I857 λ P_R *repA*(Ts); Ap^r Cm^r	13
Primer		
Δ*creB*-F†	5′-TTA GCG CGG TTC CTG TCA TGC CGT GGC GGC AAT AAC AGA GGC GAT TTA TGG TGT AGG CTG GAG CTG CTT C-3′	This study
Δ*creB*-R	5′-GCC CAG CAA CAA CCG CAT GCC GAT ACG CAT TAC AGG CCC CTC AGG CTA TAC ATA TGA ATA TCC TCC TTA G-3′	This study
kan-F	5′-CGG TGC CCT GAA TGA ACT GC-3′	This study
kan-R	5′-CGG CCA CAG TCG ATG AAT CC-3′	This study
creB-F	5′-CCT GAG GGG CCT GTA ATG-3′	This study
creB-R	5′-CTG CAC CGT ATA AAG CTC-3′	This study
arcA-F	5′-CCG AAA ATG AAA GCC AGT-3′	This study
arcA-R	5′-GAA AGT ACC CAC GAC CAA-3′	This study

[a] *, Strain obtained from the *E. coli* Genetic Stock Center (University of Yale, New Haven, CT). †, The start codon for *creB* is underlined.
[b] Cm^r, chloramphenicol resistance; Ap^r, ampicillin resistance; Km^r, kanamycin resistance.

temperature, derivatives were filtered and used for detection in a GC-MS equipment (GC · MS-QP2010; Shimadzu, Tokyo, Japan) with a DB-5MS column (30 m by 0.25 mm by 0.25 μm; Agilent Technologies, Inc., Fort Collins, CO). The apparatus parameters were set according to the method of Zhao and Shimizu (75). Briefly, the carrier gas flow was fixed at 1 ml min^{-1}, and the injection volume was 1 μl, with flow mode in split control. The oven temperature was initially held at 80°C for 2 min, and then the temperature was gradually increased to 290°C in 30 min. Interface temperature was set at 250°C and ion source temperature at 200°C. Electron impact ionization was 70 eV. To increase sensitivity, mass spectra were analyzed in selected ion recording mode.

Analytical procedures. The cell dry weight (CDW) was determined from cell pellets of 100-ml culture samples that were centrifuged for 10 min at 4°C and 10,000 × *g*, washed twice with the same volume of 150 mM NaCl, and finally dried in an oven at 55°C until constant weight was attained. Culture broth samples were centrifuged for 5 min at 13,000 × *g* in a microcentrifuge to remove the cells. The resulting supernatant was filtered through a 0.22-μm-pore-size syringe filter and stored at 4°C for high-pressure liquid chromatography analysis. Extracellular metabolites and glucose concentrations were determined by using a high-pressure liquid chromatography system (Shimadzu Scientific Instruments, Columbia, MD) equipped with a cation-exchange column (HPX-87H; Bio-Rad, Hercules, CA), a differential refractive index detector (Waters Corp., Milford, MA), and a UV-VIS detector (SPD-10A; Shimadzu Scientific Instruments). A mobile phase of 2.5 mM H_2SO_4 solution was used at a 0.6-ml min^{-1} flow rate, and the column was operated at 55°C (74).

Metabolic flux analysis and statistical analysis. To quantitatively estimate the metabolic fluxes in the main metabolic pathways, an ad hoc computer program was written in MATLAB (version 7.0; The Mathworks, Inc., Natick, MA). A metabolic network was constructed (see the Appendix), including the Embden-Meyerhof-Parnas pathway (glycolysis), the pentose phosphate (PP) pathway, the TCA cycle, the glyoxylate shunt, and fermentative pathways. This network was compiled from textbooks (25, 44) and online metabolic databases (33). Some metabolic pools, such as PPs, succinyl coenzyme A (CoA)/succinate, and isocitrate/citrate, were combined in order to further simplify the network. Reactions through phosphoenolpyruvate (PEP) carboxylase and PEP carboxykinase were combined into a bidirectional reaction, and the reaction toward oxaloacetate (OAA) production was taken as the positive reaction. We did not consider the Entner-Doudoroff pathway or the methylglyoxal bypass (from dihydroxyacetone phosphate to Pyr) in the metabolic network since glucose was used as the sole carbon source (44). Cell composition was assumed to be the same in all experimental strains, and it was derived from the work of Neidhardt et al. (44).

Flux estimation was made using a similar idea as it was previously described in literature (58, 73, 75, 76). ^{13}C-labeling experiments in *E. coli* rely on some key assumptions: (i) the various ^{13}C-labeled isotope isomers of the metabolic intermediates are in an isotopomeric steady state, (ii) ^{13}C-labeled isotope effects on biochemical reaction rates are insignificant, (iii) metabolite channeling or compartmentation is not relevant, (iv) complete biochemical knowledge of the fate of each carbon atom in the model is available or can be inferred from the obtained ^{13}C-labeling data, and (v) the stoichiometry of all biochemical reactions is well known. In this context, and by giving some arbitrary values for the free fluxes, different sets of metabolic flux distributions could be determined based on stoichiometric constraints. The GC-MS data can then be simulated based on estimated flux distribution and labeling pattern of feeding glucose. The best-fit set of flux distribution can be selected by comparing simulated GC-MS data and experimental GC-MS data. Reversible reaction fluxes were converted into net fluxes and exchange coefficients (within the range of [0,1]), as previously shown by Wiechert and de Graaf (72). Isotopomer mapping matrices were developed based on atom mapping matrices (78) to trace the isotopomer changes in the considered reactions, and they were used for isotopomer balances based on different sets of metabolic flux distributions. Isotopomer distributions in the amino acids were deduced from the isotopomer distributions of their metabolic precursors. Therefore, GC-MS signals were simulated and analyzed using the isotopomer distribution of amino acids. Flux solutions were evaluated by comparing the simulated data with the experimental data. GC-MS signals were corrected for the presence of the natural isotope abundance of atoms of H, C, N, O, Si, P, and S in the amino acids and the derivatization reagent before being used for flux analysis (68). Optimal carbon flux distribution in the bioreaction network was calculated as a best fit to all available physiological data, macromolecular biomass composition, and the afore-mentioned amino acid abundance in the biomass hydrolysate. The best-fit sets of flux distributions were found by using the genetic and direct search toolbox in MATLAB and were based on at least 100 independent calculation sets. Statistical analysis of the results was made by using a Monte Carlo approach (57, 75) and analysis of variance.

TABLE 2. Physiological parameters for the steady-state chemostat cultures at $D = 0.1\ h^{-1}$

E. coli strain	Mean ± SD[a]			
	Specific glucose consumption rate (mmol g $CDW^{-1}\ h^{-1}$)	CDW concn (g $liter^{-1}$)	$Y_{X/G}$[b] (g g^{-1})	Ethanol/acetate ratio (mol mol^{-1})
K1060 (wild-type strain)	6.88 ± 0.09	0.32 ± 0.01	0.08 ± 0.01	0.47 ± 0.03
IV1060 (Δ*creB*)	3.66 ± 0.05	0.53 ± 0.01	0.14 ± 0.02	0.35 ± 0.03
CT1062 (Δ*arcA*)	5.43 ± 0.08	0.36 ± 0.02	0.09 ± 0.01	0.91 ± 0.04
IV1062 (Δ*creB* Δ*arcA*)	3.84 ± 0.06	0.51 ± 0.03	0.15 ± 0.02	0.62 ± 0.03

[a] Results represent the mean values for at least triplicate measurements from three independent samples.
[b] $Y_{X/G}$, biomass yield on glucose.

Enzyme activity measurements. The experimental strains were grown in batch cultures in the same medium as described above, using 25 mM glucose as the sole carbon source. Microaerobic bioreactor cultures were conducted as previously described by Nikel et al. (46). Cells were harvested during exponential growth (optical density at 600 nm = 0.4 to 0.7) by centrifugation at 10,000 × *g* for 10 min at 4°C; washed twice with 100 mM Tris-HCl (pH 7.0) containing 20 mM KCl, 5 mM $MgSO_4$, 2 mM dithiothreitol, and 0.1 mM EDTA; and resuspended in the same buffer (ca. 0.5 g of wet cells in 1 ml of buffer solution). The cell suspension was stored at −20°C for 3 h, thawed on an ice bath, and disrupted by sonication. Cell extracts were obtained by centrifugation at 15,000 × *g* for 30 min and 4°C. Crude enzyme extracts were immediately used for determinations as well as to measure protein concentration (6). Enzyme activities were assayed spectrophotometrically in a thermostated recording Beckman DU 650 spectrophotometer (Beckman Coulter, Inc., Fullerton, CA). All compounds of the reaction mixture were pipetted into a cuvette of 1-cm light path, and the reaction was initiated by adding the cell extract or the substrate to give a final volume of 1 ml. Protocols for citrate synthase, isocitrate lyase, and succinate dehydrogenase (SDH) were performed essentially as described elsewhere (18, 69, 71); lactate dehydrogenase was measured as indicated by Bunch et al. (7); and acetate kinase as detailed by Dittrich et al. (17).

RESULTS

Growth parameters of *E. coli creB* and *arcA* mutants in chemostat cultures. *E. coli* strains K1060 (wild type), IV1060 (Δ*creB*), CT1062 (Δ*arcA*), and IV1062 (Δ*creB* Δ*arcA*) were grown in a glucose-limited semiaerobic chemostat culture at a dilution rate (*D*; volumetric flow rate/working volume) of 0.1 h^{-1}. This experimental setup was chosen since it was previously shown that fermentation patterns, as well as gene expression levels, showed most profound differences among wild-type *E. coli*, *creB*, and *arcA* mutants under conditions with restricted oxygen supply (3, 8, 47, 59), similar to those used in this work. The results presented here should be interpreted bearing in mind that we did not measure the actual state of perceived aerobiosis, i.e., the oxygen availability for individual cells (2). Instead, we have chosen a suitable experimental setup to describe the metabolic differences among wild-type and mutant strains under conditions of restricted oxygen supply. Chemostat cultures were repeated twice for strain IV1060 (Δ*creB*) and three times for strain IV1062 (Δ*creB* Δ*arcA*) in order to verify consistency between different runs. Steady-state biomass yields and specific glucose uptake rates of the experimental strains are shown in Table 2. Mutant strains exhibited lower glucose uptake rates. It can be seen that strains bearing the *creB* deletion showed not only higher biomass concentrations but also higher biomass yield on glucose compared to the wild-type strain or the Δ*arcA* mutant ($P < 0.05$). Carbon recovery coefficients were calculated for each experimental strain from the biomass and fermentative metabolites synthesis rates, whereas CO_2 evolution was derived from the in silico flux calculations. The good carbon recovery values shown in Table 3 confirmed the network assumptions consistency. Similarly, >90% of the reducing equivalents generated during microaerobic growth on glucose were captured in the synthesis of biomass and fermentation products (data not shown). Taken together, these results suggest an excellent closure of carbon and redox balances, thus suggesting that the most relevant metabolites and reactions were taken into account in the proposed metabolic network.

Metabolic flux analysis results. Metabolic flux distributions for the four experimental strains under study were estimated based on ^{13}C-labeling experiments at steady state. Experimental GC-MS data were corrected for the presence of the natural isotope abundance of atoms of H, C, N, O, Si, P, and S in the amino acids and derivatization reagents and compared to data simulated from flux distribution, showing that both data sets were in good agreement (data not shown). Bidirectional reactions were separated into net fluxes and exchange coefficients to avoid numerical problems during optimization (72). All fluxes were normalized to the specific glucose uptake rates (Table 2; see also reaction v_0 in the Appendix), which were considered to be 100. It can be seen from Fig. 1 that glucose internalized through the phosphotransferase system was mainly catabolized using the Embden-Meyerhof-Parnas path-

TABLE 3. Specific production rates for extracellular metabolites in steady-state chemostat cultures at $D = 0.1\ h^{-1}$

E. coli strain	Mean specific production rate (mmol g $CDW^{-1}\ h^{-1}$) ± SD[a]						Mean carbon balance[b] (%) ± SD
	Pyruvate	Lactate	Succinate	Formate	Acetate	Ethanol	
K1060 (wild-type strain)	0.08 ± 0.03	0.01 ± 0.00	0.49 ± 0.02	9.4 ± 0.4	6.2 ± 0.1	2.94 ± 0.06	93 ± 5
IV1060 (Δ*creB*)	0.09 ± 0.02	0.00 ± 0.00	0.03 ± 0.01	5.9 ± 0.2	4.1 ± 0.1	1.39 ± 0.08	91 ± 6
CT1062 (Δ*arcA*)	0.04 ± 0.01	0.41 ± 0.03	0.37 ± 0.02	9.1 ± 0.3	5.2 ± 0.2	4.64 ± 0.07	96 ± 4
IV1062 (Δ*arcA* Δ*creB*)	0.05 ± 0.03	0.09 ± 0.01	0.02 ± 0.01	6.6 ± 0.1	4.0 ± 0.1	2.51 ± 0.05	98 ± 2

[a] Results represent the mean values for at least triplicate measurements from three independent samples.
[b] CO_2 production was estimated from the flux calculations.

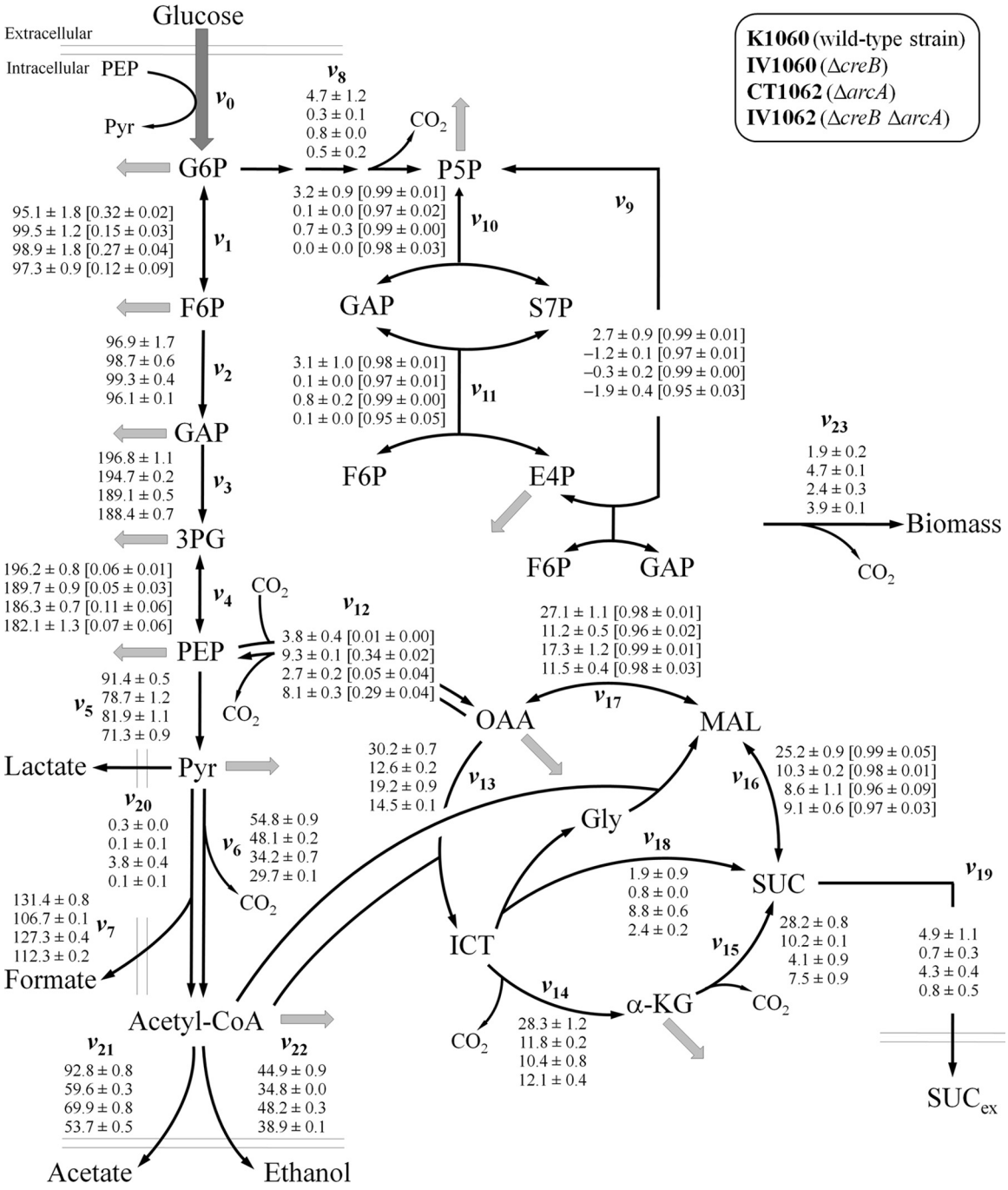

FIG. 1. Metabolic flux analysis of (from top to bottom) *E. coli* K1060 (wild-type strain), IV1060 (Δ*creB*), CT1062 (Δ*arcA*), and IV1062 (Δ*creB* Δ*arcA*) in glucose-limited continuous cultures with restricted oxygen supply at $D = 0.1\ h^{-1}$. Flux values are normalized to the specific glucose uptake rate of each strain (v_0), which was arbitrarily given the value of 100. Arrowheads indicate the assumed reaction reversibility, and interchange coefficients for these reactions are shown in brackets. Gray arrows indicate precursors for biomass synthesis. Values represent the mean of at least 100 calculations from data corresponding to three independent samples for each strain ± 90% confidence intervals. A description of each reaction can be found in the Appendix.

way (reactions v_1 to v_5). Small exchange coefficients for the reversible reactions involved show that these reactions proceeded toward Pyr generation. It is worth to mention that a slight reduction (ca. 15%) of the flux from PEP to Pyr, catalyzed by Pyr kinase (PykAF), was observed in *creB* mutants.

Under aerobic conditions, the oxidative PP pathway is used as one of the main pathways in *E. coli* to generate reducing power as NADPH (25, 44). However, flux distributions demonstrate that the oxidative PP pathway (v_8) was low for all experimental strains. All mutant strains showed almost the same fluxes through the oxidative PP pathway, and these values were >75% lower than those of wild-type K1060 ($P < 0.01$).

The oxidative PP pathway and the bidirectional nonoxidative PP pathway are both used to provide precursors for biomass synthesis (25). Reactions in the nonoxidative PP pathway exhibited exchange coefficients very close to 1, which implies that all of these reactions were highly reversible. It was reported that CreBC mutants showed a lower expression of *talA*-encoded transaldolase A (5) and, accordingly, we observed very low TalAB fluxes (v_{11}) in *creB* strains.

Comparing the flux distributions at the PEP node in the experimental strains, it can be observed that the PEP carboxylase flux (v_{12}) showed a similar trend as the biomass flux (v_{23}), which was higher for the strains bearing the *creB* mutation ($P < 0.01$) compared to those of K1060 and CT1062 (Δ*arcA*). The flux through the anaplerotic PEP carboxylase reaction was mainly used to supplement the OAA pool for biomass synthesis and reactions through the TCA cycle in the wild-type strain and its Δ*arcA* derivative. On the other hand, the reaction through PEP carboxykinase was treated as the reverse reaction of that catalyzed by PEP carboxylase. Figure 1 shows that exchange coefficients for the PEP carboxylase flux were negligible for the wild-type strain and the *arcA* mutant and slightly higher for strains carrying the *creB* deletion. In other words, fluxes through the gluconeogenic PEP carboxykinase reaction were low in the experimental strains under the semiaerobic condition tested, but higher for *creB* mutants. As stated, biomass fluxes were higher for *creB* mutants compared to the wild-type strain flux. In fact, a statistically significant increase of 2.5- and 2.1-fold was observed for strains IV1060 and IV1062, respectively ($P < 0.05$). The biomass flux for the *arcA* mutant was only slightly higher (1.3-fold) compared to that of wild-type K1060.

The flux distribution at the Pyr node largely determines the metabolic patterns in *E. coli* (9). Extracellular metabolite production rates are presented in Table 3, in which it can be observed that excreted Pyr was negligible for all experimental strains. Previous studies have suggested that ArcA represses the expression of *aceEF*, encoding subunits of the Pyr dehydrogenase (PDH) complex (38). For this reason, flux through PDH complex (v_6) should be higher for strain CT1062 compared to that of K1060, since *aceEF* expression would be derepressed. However, the flux through PDH was >13% lower in mutant strains compared to that observed for wild-type K1060 ($P < 0.05$). In strain IV1062 (bearing the *creB* and *arcA* deletions) this flux was 46% lower, suggesting that the CreBC system may exert some modulation on *aceEF* expression together with the ArcAB system since it seems that there is an additive effect of both regulatory systems. However, it is important to note that the difference observed in the PDH flux could also be an indirect effect of changes in other fluxes as a consequence of variations in the intracellular metabolite pools. Therefore, more studies are needed to clarify the possible transcriptional regulation of *aceEF* by Cre. On the other hand, the Pfl flux (v_7) was slightly lower for the *arcA* mutant ($P < 0.05$). This is consistent with previous studies reporting that *pflAB* expression is activated by ArcA (1, 3, 61). Lower Pfl fluxes were observed in strains bearing the *creB* mutation: for IV1060 (Δ*creB*), the Pfl flux was ca. 19% lower than that of K1060, while for IV1062 (Δ*arcA* Δ*creB*) a reduction of ca. 15% was observed. In addition, it should be noted that conversion of Pyr into acetyl-CoA may also occur through the reactions catalyzed by TdcE (56) or modulated by YfiD, particularly in a Δ*arcA* background (77).

Flux toward lactate synthesis (v_{20}) was almost zero for the wild-type strain and the strains bearing the *creB* mutation. Nevertheless, it was observed that the *arcA* mutant showed a 12.7-fold increase in this flux ($P < 0.01$). It was previously shown that *ldhA* expression is derepressed in a Δ*arcA* background (59). However, we did not detect significant lactate synthesis in supernatants of the double-mutant cultures and, accordingly, fermentative lactate dehydrogenase (LdhA) flux in this strain was negligible. This result is in agreement with the higher PEP carboxylase fluxes observed in *cre* mutants, suggesting that PEP is deviated toward the TCA cycle reactions. It is possible to speculate that the higher LdhA flux in the Δ*arcA* mutant could be a consequence of higher Pyr concentration and reducing equivalents accumulation.

Based in the stoichiometric constraints of the model, lower phosphotransacetylase (Pta) and acetate kinase (AckA) fluxes (v_{21}), conducive to extracellular acetate, were observed for the three mutant strains compared to those of wild-type K1060. This behavior was particularly evident for IV1062, the double mutant strain (showing ca. 42% reduction in acetate synthesis [$P < 0.01$]), suggesting an additive effect of mutations in both ArcAB and CreBC on Pta-AckA fluxes. These results are in good agreement with the reported reduction of *pta-ackA* expression in a *creC*::*kan* mutant of *E. coli* DH5α (5), and in a Δ*arcA* mutant of *E. coli* MG1655 (61). It is worth mentioning that conversion of Pyr to extracellular acetate is usually assumed to occur through the reactions catalyzed by PDH and/or Pfl, Pta, and AckA, but it may also arise from Pyr oxidase activity (PoxB) in one step. The latter reaction could be active in acetate-producing cultures (17). Both reaction sequences create the same ^{13}C-labeling pattern, so that our present analysis cannot differentiate between the two routes. However, the flux results are not affected by the potential presence of PoxB.

Compared to the wild-type strain, the flux toward ethanol synthesis (v_{22}) was lower for strains carrying the *creB* mutation but higher for CT1062 (Δ*arcA*). In this case, a higher ethanologenic flux could suggest a higher redox potential for the *arcA* mutant. Even when a direct effect of ArcA or CreB was not demonstrated for *adhE*, it is well established that *E. coli* synthesizes ethanol to maintain the redox balance (9). Ethanol/acetate molar ratios (Table 2) also show that strains carrying the *arcA* deletion exhibit a highly reducing intracellular environment.

It can be seen in Fig. 1 that the TCA reactions still worked as a cycle under the experimental conditions tested, instead of two branches. All of the TCA cycle reactions were substantially lower in the mutant strains. Fluxes through the later part of the cycle include the reactions through SDH, fumarate reductase, and malate dehydrogenase. Exchange coefficients values (which were >0.95 for v_{16} and v_{17}) indicate that the reactions of fumarase (which converts fumarate into malate) and malate dehydrogenase (which converts malate into OAA) are highly reversible under the experimental semiaerobic conditions. Previous studies indicated that expression of genes encoding TCA cycle enzymes, such as *gltA* and *icd*, are repressed by ArcA under microaerobic conditions (60). However, similar to what was observed for the PDH fluxes, fluxes through citrate synthase (GltA, v_{13}) and isocitrate dehydrogenase (v_{14}) were

TABLE 4. In vitro enzyme activities in batch cultures of wild-type and mutant strains

E. coli strain	Avg enzyme sp act (μmol min^{-1} mg of $protein^{-1}$) ± SD[a] for:				
	Citrate synthase	Isocitrate lyase	Succinate dehydrogenase	Lactate dehydrogenase	Acetate kinase
K1060 (wild-type strain)	0.98 ± 0.02	0.09 ± 0.01	0.17 ± 0.01	0.47 ± 0.06	1.35 ± 0.03
IV1060 (Δ*creB*)	0.43 ± 0.05	0.05 ± 0.02	0.09 ± 0.03	0.09 ± 0.02	0.38 ± 0.05
CT1062 (Δ*arcA*)	0.59 ± 0.03	0.27 ± 0.01	0.11 ± 0.02	1.02 ± 0.03	0.76 ± 0.02
IV1062 (Δ*creB* Δ*arcA*)	0.48 ± 0.04	0.16 ± 0.04	0.08 ± 0.03	0.06 ± 0.02	0.24 ± 0.09

[a] Values represent averages of duplicate measurements from two independent cultures.

lower in all mutant strains. On the other hand, the glyoxylate shunt reactions (v_{18}), consisting of isocitrate lyase (AceA) and malate synthase (AceB and GlcB), were found to be active in strain CT1062 (*arcA* mutant), which showed a flux through these reactions ~5-fold higher than that of the wild-type strain ($P < 0.01$), a finding in good agreement with the reported repression of *aceBAK* by ArcA under conditions of restricted oxygen supply (30). The glyoxylate shunt was also active in strain IV1062 (*creB arcA* double mutant) but to a lesser extent (~1.3-fold increase compared to the wild-type strain [$P < 0.05$]). Residual activity through the glyoxylate shunt was also present in K1060 and IV1060, as demonstrated for wild-type *E. coli* strains under glucose limitation (39). Taking into account the lower TCA cycle fluxes in the mutant strains, significant succinate excretion (v_{19}) was only detected for the wild-type strain and its Δ*arcA* derivative, which seems to be mostly provided by the glyoxylate shunt reactions.

Enzymatic activities in *arcA* and *creB* mutants. In order to further investigate the regulation mechanisms that could cause the flux changes, the activities of several enzymes which showed significant differences by metabolic flux analysis were determined. We conducted microaerobic batch cultures of the wild-type strain and its *cre* and *arc* derivatives, and samples were taken during the exponential phase of growth for in vitro measurements of citrate synthase, isocitrate lyase, SDH, lactate dehydrogenase, and acetate kinase activities (Table 4). In the middle of the exponential phase, bacterial cells can be considered to be in a quasi-steady state (55, 73); thus, the enzyme activities can be compared to some extent with results obtained through fluxome analysis. Moreover, dissolved oxygen concentrations in the exponential cultures were roughly similar to those used in chemostat cultivation (data not shown).

It can be observed that the enzyme activities of the mutant strains followed the same trend as the corresponding fluxes shown in Fig. 1, suggesting a similar regulatory pattern. GltA was found to be mainly active in K1060, while strains carrying the *creB* deletion had a ca. 50% reduction in this activity. The *arc* mutant showed a slightly lower GltA activity compared to K1060. A similar behavior was observed for SDH. Again, the highest SDH activity was registered in the wild-type strain. On the other hand, CT1062 (Δ*arcA*) showed the highest isocitrate lyase activity under microaerobic conditions (threefold higher than that of the wild-type strain). Also, fermentative LdhA activity was 2.2-fold higher for CT1062, which correlates with the high extracellular lactate flux obtained for this strain (Table 3). The activity of AckA, an enzyme for which CreBC-dependent regulation is well established (5, 47), was also assayed. As expected, strains IV1060 and IV1062 (*creB* mutants) exhibited >70% lower activity than that of wild-type K1060. AckA activity was also low for CT1062 (ca. 44% lower than the activity in K1060) and reflects the funneling of acetyl-CoA toward ethanol synthesis instead of acetate formation, which is in good agreement with the ethanol/acetate ratio of this strain in chemostat cultures (Table 2).

Even when our results show a similar trend in some metabolic fluxes and enzyme activities associated with them, it is appropriate to mention that in vivo activity is subjected to a wide variety of regulatory mechanisms. Among them, one particularly relevant mechanism is allosteric regulation. Differences in the enzyme activity level in the mutant strains (and therefore, in the corresponding metabolic fluxes) could be the consequence of several metabolic and regulatory phenomena which are not directly related with transcriptional control exerted by the global regulators under study. Nevertheless, the good correlation we found between in vivo catabolic fluxes and in vitro enzyme activity suggests a similar regulatory pattern in both parameters.

DISCUSSION

In the present study, variations resulting from different mutations in the global regulators CreBC and ArcAB (controlling responses to carbon source and oxygen availability) were systematically analyzed by combined physiological and fluxome analysis. This objective was attained by quantifying intracellular metabolic flux distributions in a wild-type strain of *E. coli*, a *creB* mutant, an *arcA* mutant, and a *creB arcA* double mutant by means of ^{13}C-labeling experiments under microaerobic conditions. Metabolic flux analysis was demonstrated to be an important and useful tool for holistic interpretation of the central metabolism since deletion of regulatory genes may affect the entire cellular metabolite pattern in a difficult-to-predict fashion. This in turn can affect the activity of various other enzymes and pathways, being especially relevant when considering the effects of combinations of global regulators under conditions where it is difficult to know the contributions of each one on a cell culture. For instance, it can be seen in Table 2 that the ethanol/acetate ratios are changed in different directions by Arc and Cre, so the phenotypic properties in the double mutant are not easy to predict.

Deletion of either *arcA* and/or *creB* did not significantly affect the fluxes toward PEP, while the flux distribution at the PEP, Pyr, and acetyl-CoA nodes were affected by both CreBC and ArcAB regulatory systems. Lower fluxes were registered for all mutant strains in both the oxidative and nonoxidative

PP pathways. From a physiological perspective, high fluxes through the oxidative PP pathway under microaerobic conditions appear unreasonable because the cell is not able to reoxidize concomitantly formed NADPH; however, an additive effect of CreB and ArcA seems to operate on this pathway. The effect of the CreBC system on key points of the nonoxidative PP pathway under aerobic conditions was previously discussed (5).

The flux distribution at the Pyr node results from competition between lactate synthesis through LdhA activity, and acetyl-CoA synthesis by PDH and/or Pfl. Although the acetyl-CoA pool was mainly supplemented by the reaction through Pfl, both Pfl and PDH were active under the 2.5% O_2-in-N_2 condition used in the present study. Since the formate formed by Pfl would not be decomposed at neutral pH (77), the Pfl flux would correlate with the extracellular formate fluxes. Small differences observed in this correlation could be attributed to the activity of formate-hydrogen lyase, which catalyzes the conversion of formate into CO_2 and H_2 (9). Similar and negligible LdhA fluxes were observed for strains K1060 (wild type), IV1060 (Δ*creB*), and IV1062 (Δ*creB* Δ*arcA*). However, *arcA* disruption gave rise to an important increase in LdhA flux, most probably to maintain the intracellular carbon skeletons and redox balance. When LdhA activity was determined in exponential cultures a high activity was observed for strain CT1062, which correlates well with the flux distribution obtained in silico.

The lower fluxes through PDH in cultures of *arcA* strains compared to the wild-type strain are in contrast to the previously reported repression effect of ArcA on *aceEF* expression (38). Indeed, Shalel-Levanon et al. (61) demonstrated that *aceE* expression level was higher in an *arcA* strain under conditions similar to those used in this work. Since the PDH enzyme is inhibited by NADH, and a higher ethanol/acetate redox ratio [which also reflects a higher NAD(P)H/NAD(P)$^+$ ratio] was observed in strains CT1062 and IV1062 compared to the wild-type strain, it seems that the lower PDH fluxes resulted from a reduced activity of the PDH complex caused by the redox environment, as suggested by Snoep et al. (62). We also observed a reduced PDH flux in strain IV1060, carrying the *creB* deletion, which is not directly attributable to a reducing intracellular redox environment. No previous reports have described a regulation of PDH by the CreBC system, and this possibility remains to be elucidated.

As observed by Avison et al. (5), a reduction in Pta-AckA activity in *creC* mutants grown in minimal medium with glucose as the sole carbon source would correlate with higher intracellular levels of Pyr, a phenomenon that was also demonstrated in *E. coli* W3110 *pta*::Tn*10* mutants (11). Judging by the flux distribution and the enzymatic activity determinations, lower conversion of acetyl-CoA into acetate takes place in *creB* mutant strains. As stated above, when reducing equivalents are in excess, Pyr can be converted into lactate through NADH-dependent LdhA (as was the case for CT1062, the *arcA* mutant). Zhu et al. (76) previously showed that higher fluxes toward lactate synthesis in an *arcA* background can be attributed to the lower conversion of Pyr into acetyl-CoA and, at the same time, a reducing redox environment. Pyr utilization is important for maintenance of carbon fluxes because when its concentration reaches a threshold value, PEP synthesis is inhibited and growth on phosphotransferase system sugars is impaired (11, 37), among other metabolic effects. We observed that conversion of PEP into Pyr was lower in *creB* mutants and, at the same time, glucose uptake rates were ca. 45% lower (Table 2), a result that is in good agreement with the documented modulation of the phosphotransferase system activity. Similarly, both acetate and ethanol fluxes were concomitantly reduced in *creB* mutants, which could lead to acetyl-CoA accumulation. A well-documented effect of intracellular acetyl-CoA build-up is the allosteric activation of PEP carboxylase (32), a situation that would account, at least in part, for the higher fluxes observed for this reaction in strains IV1060 and IV1062. However, it should be stressed that the lower catabolic rates observed in the mutants can be also due to a wide range of effects, e.g., changes in intracellular metabolite pools and/or fluxes. On the other hand, Pyr is the main stoichiometric contributor in the reaction conducive to biomass (see the Appendix). Since lower fluxes through LdhA, PDH, and Pfl were observed for *creB* mutants, it is tempting to speculate that perhaps more Pyr is being drained to biomass building block synthesis under our experimental conditions, which would correlate with the higher biomass yields and fluxes observed for strains IV1060 and IV1062. A similar conclusion was suggested from results derived from a theoretical analysis of carbon partitioning between biomass synthesis and by-products excretion (16). In addition, considering the stoichiometric balance at the acetyl-CoA node, it can be seen that a higher availability of this precursor is also evident in strains IV1060 and IV1062 which could be eventually funneled into biomass synthesis.

The underlying mechanism for potentially higher energetic efficiency in *creB* mutants is unknown. It should be kept in mind that metabolic perturbations are widely possible in mutants for global regulators, and some of them could not be considered in our biochemical network but certainly can influence cellular parameters such as biomass yield. Under semiaerobic conditions, besides ATP generation in the fermentative metabolic pathways, an important contribution of ATP is obtained through respiration. Since the P/O ratio greatly varies in different organisms under different conditions (45), ATP generation through respiratory chain activity cannot be directly calculated. Besides these observations, it should be realized that a higher intracellular ATP concentration is not necessarily the main reason for higher biomass yield on substrate. A recent report showed the opposite trend in glucose-limited chemostat cultures of *E. coli* (35). Accordingly, it has been previously demonstrated that the distribution of carbon skeletons, rather than ATP availability, seems to be the most important factor modulating the biomass yield of *E. coli* on substrate under conditions of restricted oxygen supply (67). Similar conclusions were reached in yeasts, such as *Saccharomyces cerevisiae* (63) and *Candida utilis* (70). For instance, it has been demonstrated that higher PEP carboxylase is directly correlated with enhanced biomass yield on substrate (12), although no significant changes in ATP availability can be anticipated. In the present study, the flux through this anaplerotic enzyme was higher for *creB* mutants, directly correlating with the flux from macromolecular precursors to biomass and the biomass yield on substrate. Our hypothesis is that at a given ATP availability differences in the carbon fluxes distribution may significantly alter the biomass yield on substrate. We are currently conducting

experiments aimed at providing a quantitative correlation between catabolic and energetic efficiency in *creB* mutants.

Recent evidence suggests that transcriptional control of fluxes is often specific for a particular metabolic pathway in a highly condition-dependent fashion (21, 24, 29, 59). Since fluxes are the integrated consequence of all regulatory and biochemical interactions within the metabolic network, it is not surprising that our results significantly deviate from previous conclusions exclusively based on genetic evidence. In agreement with the observations of Perrenoud and Sauer (52), we found that TCA cycle reactions operate in a substantially cyclic fashion under conditions of restricted oxygen supply instead of the usually proposed two-branch pathway (42). Even when such a cyclic activity was detected, all TCA cycle fluxes in mutant strains were reduced compared to those of wild-type K1060. The in vitro GltA and SDH activities followed the same trend observed in the flux distribution. A similar result was observed by Shalel-Levanon et al. (59), demonstrating that at oxygen concentrations in the bioreactor headspace ranging from 1 to 2.5%, succinate fluxes were higher for a wild-type *E. coli* strain compared to Δ*arcA* and Δ*arcA* Δ*fnr* mutants. The authors of that study also found a significant inhibition of the TCA cycle reactions by a high NADH/NAD^+ ratio in the mutant strains.

It is noteworthy that during chemostat cultures of IV1062, the Δ*creB* Δ*arcA* mutant, steady-state conditions were attained only after approximately 10 residence times (for the wild-type strain and its single-mutation derivatives it took about 7 residence times). This particular behavior, which was consistently reproduced in three independent cultivations, could be due to a poor metabolic regulation in the absence of two global regulators under our carbon-limited conditions with restricted oxygen supply. The possibility that mutations in other genes, namely, *rpoS*, encoding the general stress response σ^S factor (28), could arise in subpopulations of our cultures during such a long cultivation time cannot be ruled out (22, 49); however, homogeneous colony morphology was found after plating dilutions of these cultures, and no qualitative differences in glycogen accumulation, an indirect indicator of *rpoS* partial and null mutations (27), were detected after iodine staining (data not shown).

Metabolic flux analysis was recently performed using glucose-limited chemostat cultures under aerobic conditions for various regulatory mutants, among them, Δ*creB*::*kan*, Δ*creC*::*kan*, Δ*arcA*::*kan*, and Δ*arcB*::*kan* derivatives of *E. coli* BW25113 (43). Interestingly, a higher glucose uptake rate was observed for *creB* and *creC* mutants than for BW25113. Besides these observations, no significant differences were observed among the strains under study, and it was concluded that under the conditions tested, the above-mentioned mutations are phenotypically silent. Oshima et al. (50) also considered that the CreBC system does not exert an important regulation on gene expression under aerobic conditions, as judged from results of microarray transcriptomic experiments using *E. coli* mutants in all known two-component signal transduction systems. However, it is important to stress that both CreBC and ArcAB regulatory systems seem to exert an important influence on central metabolism in microaerobiosis (3, 8, 48, 59), and this could be the reason for which no differences were observed under aerobic conditions of growth. Finally, and taking into account that both global regulatory systems exert an important influence on carbon and redox balances, manipulation of the genes for these regulators could provide a relevant tool for modulation of central metabolism and reducing power availability aimed at biotechnological purposes.

APPENDIX

The components of the metabolic network used for flux calculation were as follows.

v_0: glucose + PEP → G6P + Pyr.
v_1: G6P ↔ F6P.
v_2: F6P → 2 GAP.
v_3: GAP → 3PG.
v_4: 3PG ↔ PEP.
v_5: PEP → Pyr.
v_6: Pyr → acetyl-CoA + CO_2.
v_7: Pyr → acetyl-CoA + formate.
v_8: G6P → P5P + CO_2.
v_9: P5P + E4P ↔ F6P + GAP.
v_{10}: 2 P5P ↔ GAP + S7P.
v_{11}: GAP + S7P ↔ F6P + E4P.
v_{12}: PEP + CO_2 ↔ OAA.
v_{13}: acetyl-CoA + OAA → ICT.
v_{14}: ICT → α-KG + CO_2.
v_{15}: α-KG → SUC + CO_2.
v_{16}: SUC ↔ MAL.
v_{17}: MAL ↔ OAA.
v_{18}: ICT + acetyl-CoA → MAL + SUC.
v_{19}: SUC → SUC_{ex}.
v_{20}: Pyr → lactate.
v_{21}: acetyl-CoA → acetate.
v_{22}: acetyl-CoA → ethanol.
v_{23}: 0.133 G6P + 0.071 F6P + 0.107 GAP + 1.661 3PG + 0.964 PEP + 3.635 Pyr + 2.523 acetyl-CoA + 0.535 P5P + 0.456 E4P + 1.61 α-KG + 1.786 OAA → biomass + 2.828 CO_2.

Abbreviations: Pyr, pyruvate; G6P, glucose 6-phosphate; F6P, fructose 6-phosphate; GAP, glyceraldehyde 3-phosphate; 3PG, 3-phosphoglycerate; P5P, pentose 5-phosphate; E4P, erythrose 4-phosphate; S7P, sedoheptulose 7-phosphate; ICT, isocitrate; α-KG, α-ketoglutarate; SUC, succinate; SUC_{ex}, extracellular succinate; MAL, malate.

ACKNOWLEDGMENTS

This study was supported by grants from the National Science Foundation (BES-0420840; CBET-0828516) and from the Consejo Nacional de Investigaciones Científicas y Técnicas (CONICET) of Argentina. P.I.N. is a graduate student fellow of CONICET. While working at the Department of Biochemistry and Cell Biology of Rice University, P.I.N. was partially supported by CONICET and the American Society for Microbiology (ASM), through an ASM Fellowship for Latin American students. B.S.M. is a CONICET researcher.

The excellent technical assistance by Mary L. Harrison is gratefully acknowledged.

REFERENCES

1. **Alexeeva, S., B. de Kort, G. Sawers, K. J. Hellingwerf, and M. J. Teixeira de Mattos.** 2000. Effects of limited aeration and of the ArcAB system on intermediary pyruvate catabolism in *Escherichia coli*. J. Bacteriol. **182:**4934–4940.
2. **Alexeeva, S., K. J. Hellingwerf, and M. J. Teixeira de Mattos.** 2002. Quantitative assessment of oxygen availability: perceived aerobiosis and its effect on flux distribution in the respiratory chain of *Escherichia coli*. J. Bacteriol. **184:**1402–1406.
3. **Alexeeva, S., K. J. Hellingwerf, and M. J. Teixeira de Mattos.** 2003. Requirement of ArcA for redox regulation in *Escherichia coli* under microaerobic but not anaerobic or aerobic conditions. J. Bacteriol. **185:**204–209.
4. **Amemura, M., K. Makino, H. Shinagawa, and A. Nakata.** 1986. Nucleotide sequence of the *phoM* region of *Escherichia coli*: four open reading frames may constitute an operon. J. Bacteriol. **168:**294–302.
5. **Avison, M. B., R. E. Horton, T. R. Walsh, and P. M. Bennett.** 2001. *Escherichia coli* CreBC is a global regulator of gene expression that responds to growth in minimal media. J. Biol. Chem. **276:**26955–26961.

6. **Bradford, M. M.** 1976. A rapid and sensitive method for the quantitation of microgram quantities of protein utilizing the principle of protein-dye binding. Anal. Biochem. **72:**248–254.
7. **Bunch, P. K., F. Mat-Jan, N. A. Lee, and D. P. Clark.** 1997. The *ldhA* gene encoding the fermentative lactate dehydrogenase of *Escherichia coli*. Microbiology **143:**187–195.
8. **Cariss, S. J. L., A. E. Tayler, and M. B. Avison.** 2008. Defining the growth conditions and promoter-proximal DNA sequences required for activation of gene expression by CreBC in *Escherichia coli*. J. Bacteriol. **190:**3930–3939.
9. **Clark, D. P.** 1989. The fermentation pathways of *Escherichia coli*. FEMS Microbiol. Rev. **5:**223–234.
10. **Cotter, P. A., and R. P. Gunsalus.** 1992. Contribution of the *fnr* and *arcA* gene products in coordinate regulation of cytochrome *o* and days oxidase (*cyoABCDE* and *cydAB*) genes in *Escherichia coli*. FEMS Microbiol. Lett. **70:**31–36.
11. **Chang, D. E., S. Shin, J. S. Rhee, and J. G. Pan.** 1999. Acetate metabolism in a *pta* mutant of *Escherichia coli* W3110: importance of maintaining acetyl coenzyme A flux for growth and survival. J. Bacteriol. **181:**6656–6663.
12. **Chao, Y. P., and J. C. Liao.** 1993. Alteration of growth yield by overexpression of phosphoenolpyruvate carboxylase and phosphoenolpyruvate carboxykinase in *Escherichia coli*. Appl. Environ. Microbiol. **59:**4261–4265.
13. **Cherepanov, P. P., and W. Wackernagel.** 1995. Gene disruption in *Escherichia coli*: Tc^r and Km^r cassettes with the option of Flp-catalyzed excision of the antibiotic-resistance determinant. Gene **158:**9–14.
14. **Datsenko, K., and B. L. Wanner.** 2000. One-step inactivation of chromosomal genes in *Escherichia coli* K-12 using PCR products. Proc. Natl. Acad. Sci. USA **97:**6640–6645.
15. **Dauner, M., and U. Sauer.** 2000. GC-MS analysis of amino acids rapidly provides rich information for the isotopomer balancing. Biotechnol. Prog. **16:**642–649.
16. **Delgado, J., and J. C. Liao.** 1997. Inverse flux analysis for reduction of acetate excretion in *Escherichia coli*. Biotechnol. Prog. **13:**361–367.
17. **Dittrich, C. R., G. N. Bennett, and K. Y. San.** 2005. Characterization of the acetate-producing pathways in *Escherichia coli*. Biotechnol. Prog. **21:**1062–1067.
18. **Dixon, G. H., and H. L. Kornberg.** 1959. Assay methods for key enzymes of the glyoxylate cycle. Biochem. J. **73:**3–10.
19. **Drapal, N., and G. Sawers.** 1995. Promoter 7 of the *E. coli pfl* operon is a major determinant in the anaerobic regulation of expression by ArcA. J. Bacteriol. **177:**5338–5341.
20. **Elias, W. P., J. R. Czeczulin, I. R. Henderson, L. R. Trabulsi, and J. P. Nataro.** 1999. Organization of biogenesis genes for aggregative adherence fimbria II defines a virulence gene cluster in enteroaggregative *Escherichia coli*. J. Bacteriol. **181:**1779–1785.
21. **Emmerling, M., M. Dauner, A. Ponti, J. Fiaux, M. Hochuli, T. Szyperski, K. Wüthrich, J. A. Bailey, and U. Sauer.** 2002. Metabolic flux responses to pyruvate kinase knockout in *Escherichia coli*. J. Bacteriol. **184:**152–164.
22. **Ferenci, T.** 2008. Bacterial physiology, regulation and mutational adaptation in a chemostat environment. Adv. Microb. Physiol. **53:**169–229.
23. **Georgellis, D., O. Kwon, and E. C. C. Lin.** 2001. Quinones as the redox signal for the *arc* two-component system of bacteria. Science **292:**2314–2316.
24. **Gosset, G., Z. Zhang, S. Nayyar, W. A. Cuevas, and M. H. Saier, Jr.** 2004. Transcriptome analysis of Crp-dependent catabolite control of gene expression in *Escherichia coli*. J. Bacteriol. **186:**3516–3524.
25. **Gottschalk, G.** 1986. Bacterial metabolism. Springer Verlag, New York, NY.
26. **Harder, W., and L. Dijkhuizen.** 1983. Physiological responses to nutrient limitation. Annu. Rev. Microbiol. **37:**1–24.
27. **Hengge-Aronis, R., and D. Fischer.** 1992. Identification and molecular analysis of *glgS*, a novel growth-phase-regulated and *rpoS*-dependent gene involved in glycogen synthesis in *Escherichia coli*. Mol. Microbiol. **6:**1877–1886.
28. **Hengge-Aronis, R.** 2000. The general stress response in *Escherichia coli*, p. 161–178. *In* G. Storz and R. Hengge-Aronis (ed.), Bacterial stress responses. ASM Press, Washington, DC.
29. **Hua, Q., C. Yang, T. Oshima, H. Mori, and K. Shimizu.** 2004. Analysis of gene expression in *Escherichia coli* in response to changes of growth-limiting nutrient in chemostat cultures. Appl. Environ. Microbiol. **70:**2354–2366.
30. **Iuchi, S., and E. C. C. Lin.** 1988. *arcA* (*dye*), a global regulatory gene in *Escherichia coli* mediating repression of enzymes in aerobic pathways. Proc. Natl. Acad. Sci. USA **85:**1888–1892.
31. **Iuchi, S., V. Chepuri, H. A. Fu, R. B. Gennis, and E. C. C. Lin.** 1990. Requirement for terminal cytochromes in generation of the aerobic signal for the *arc* regulatory system in *Escherichia coli*: study utilizing deletions and *lac* fusions of *cyo* and *cyd*. J. Bacteriol. **172:**6020–6025.
32. **Izui, K., M. Taguchi, M. Morikawa, and H. Katsuki.** 1981. Regulation of *Escherichia coli* phosphoenolpyruvate carboxylase by multiple effectors in vivo. II. Kinetic studies with a reaction system containing physiological concentrations of ligands. J. Biochem. **90:**1321–1331.
33. **Karp, P. D., M. Riley, M. H. Saier, Jr., I. T. Paulsen, S. M. Paley, and A. Pellegrini-Toole.** 2000. The EcoCyc and MetaCyc databases. Nucleic Acids Res. **28:**56–59.
34. **Kwon, O., D. Georgellis, and E. C. C. Lin.** 2000. Phosphorelay as the sole physiological route of signal transmission by the *arc* two-component system of *Escherichia coli*. J. Bacteriol. **182:**3858–3862.
35. **Kwon, Y. D., S. Y. Lee, and P. Kim.** 2008. A physiology study of *Escherichia coli* overexpressing phosphoenolpyruvate carboxykinase. Biosci. Biotechnol. Biochem. **72:**1138–1141.
36. **Lara, A. R., E. Galindo, O. T. Ramírez, and L. A. Palomares.** 2006. Living with heterogeneities in bioreactors: understanding the effect of environmental gradients in cells. Mol. Biotechnol. **34:**355–381.
37. **Liao, J. C., S. Y. Hou, and Y. P. Chao.** 1996. Pathway analysis, engineering, and physiological considerations for redirecting central metabolism. Biotechnol. Bioeng. **52:**129–140.
38. **Lynch, A. S., and E. C. C. Lin.** 1996. Responses to molecular oxygen, p. 1526–1538. *In* F. C. Neidhardt, R. Curtiss III, J. L. Ingraham, E. C. C. Lin, K. B. Low, B. Magasanik, W. S. Reznikoff, M. Riley, M. Schaechter, and H. E. Umbarger (ed.), *Escherichia coli* and *Salmonella*: cellular and molecular biology, 2nd ed., vol. 1. ASM Press, Washington, DC.
39. **Maharjan, R. P., P. L. Yu, S. Seeto, and T. Ferenci.** 2005. The role of isocitrate lyase and the glyoxylate cycle in *Escherichia coli* growing under glucose limitation. Res. Microbiol. **156:**178–183.
40. **Malpica, R., B. Franco, C. Rodríguez, and D. Georgellis.** 2004. Identification of a quinone-sensitive redox switch in the ArcB sensor kinase. Proc. Natl. Acad. Sci. USA **101:**13318–13323.
41. **Martínez-Antonio, A., and J. Collado-Vives.** 2003. Identifying global regulators in transcriptional regulatory networks in bacteria. Curr. Opin. Microbiol. **6:**482–489.
42. **Nam, T. W., Y. H. Park, H. J. Jeong, S. Ryu, and Y. J. Seok.** 2005. Glucose repression of the *Escherichia coli sdhCDAB* operon revisited: regulation by the CRP-cAMP complex. Nucleic Acids Res. **33:**6712–6722.
43. **Nanchen, A., A. Schicker, O. Revelles, and U. Sauer.** 2008. Cyclic AMP-dependent catabolite repression is the dominant control mechanism of metabolic fluxes under glucose limitation in *Escherichia coli*. J. Bacteriol. **190:**2323–2330.
44. **Neidhardt, F. C., J. L. Ingraham, and M. Schaechter.** 1990. Physiology of the bacterial cell: a molecular approach. Sinauer Associates, Sunderland, MA.
45. **Neijssel, O. M., and M. J. Teixeira de Mattos.** 1994. The energetics of bacterial growth: a reassessment. Mol. Microbiol. **13:**179–182.
46. **Nikel, P. I., M. J. Pettinari, M. A. Galvagno, and B. S. Méndez.** 2006. Poly(3-hydroxybutyrate) synthesis by recombinant *Escherichia coli arcA* mutants in microaerobiosis. Appl. Environ. Microbiol. **72:**2614–2620.
47. **Nikel, P. I., A. de Almeida, M. J. Pettinari, and B. S. Méndez.** 2008. The legacy of HfrH: mutations in the two-component system CreBC are responsible for the unusual phenotype of an *Escherichia coli arcA* mutant. J. Bacteriol. **190:**3404–3407.
48. **Nikel, P. I., M. J. Pettinari, M. C. Ramirez, M. A. Galvagno, and B. S. Méndez.** 2008. *Escherichia coli arcA* mutants: metabolic profile characterization of microaerobic cultures using glycerol as a carbon source. J. Mol. Microbiol. Biotechnol. **15:**48–54.
49. **Notley-McRobb, L., T. King, and T. Ferenci.** 2002. *rpoS* mutations and loss of general stress resistance in *Escherichia coli* populations as a consequence of conflict between competing stress responses. J. Bacteriol. **184:**806–811.
50. **Oshima, T., H. Aiba, Y. Masuda, S. Kanaya, M. Sugiura, B. L. Wanner, H. Mori, and T. Mizuno.** 2002. Transcriptome analysis of all two-component regulatory system mutants of *Escherichia coli* K-12. Mol. Microbiol. **46:**281–291.
51. **Overath, P., H. U. Schairer, and W. Stoffel.** 1970. Correlation of in vivo and in vitro phase transitions of membrane lipids in *Escherichia coli*. Proc. Natl. Acad. Sci. USA **67:**606–612.
52. **Perrenoud, A., and U. Sauer.** 2005. Impact of global transcriptional regulation by ArcA, ArcB, Cra, Crp, Cya, Fnr, and Mlc on glucose catabolism in *Escherichia coli*. J. Bacteriol. **187:**3171–3179.
53. **Roeder, W., and R. Somerville.** 1979. Cloning the *trpR* gene. Mol. Gen. Genet. **176:**361–368.
54. **Salmon, K. A., S. P. Hung, N. R. Steffen, R. Krupp, P. Baldi, G. W. Hatfield, and R. P. Gunsalus.** 2005. Global gene expression profiling in *Escherichia coli* K-12: effects of oxygen availability and ArcA. J. Biol. Chem. **280:**15084–15096.
55. **Sauer, U., D. R. Lasko, J. Fiaux, M. Hochuli, R. Glaser, T. Szyperski, K. Wüthrich, and J. A. Bailey.** 1999. Metabolic flux ratio analysis of genetic and environmental modulations of *Escherichia coli* central carbon metabolism. J. Bacteriol. **181:**6679–6688.
56. **Sawers, G., C. Heβlinger, N. Muller, and M. Kaiser.** 1998. The glycyl radical enzyme TdcE can replace pyruvate-formate lyase in glucose fermentation. J. Bacteriol. **180:**3509–3516.
57. **Schmidt, K., A. Marx, A. A. de Graaf, W. Wiechert, H. Sahm, J. Nielsen, and J. Villadsen.** 1998. ^{13}C tracer experiments and metabolite balancing for metabolic flux analysis: comparing two approaches. Biotechnol. Bioeng. **58:**254–257.
58. **Schmidt, K., L. C. Nørregaard, B. Pedersen, A. Meissner, J. O. Duus, J. O. Nielsen, and J. Villadsen.** 1999. Quantification of intracellular metabolic fluxes from fractional enrichment and ^{13}C-^{13}C coupling constraints on the isotopomer distribution in labeled biomass components. Metab. Eng. **1:**166–179.

59. **Shalel-Levanon, S., K. Y. San, and G. N. Bennett.** 2005. Effect of oxygen on the *Escherichia coli* ArcA and FNR regulation systems and metabolic responses. Biotechnol. Bioeng. **89:**556–564.
60. **Shalel-Levanon, S., K. Y. San, and G. N. Bennett.** 2005. Effect of oxygen, and ArcA and FNR regulators on the expression of genes related to the electron transfer chain and the TCA cycle in *Escherichia coli*. Metab. Eng. **7:**364–374.
61. **Shalel-Levanon, S., K. Y. San, and G. N. Bennett.** 2005. Effect of ArcA and FNR on the expression of genes related to the oxygen regulation and the glycolysis pathway in *Escherichia coli* under microaerobic growth conditions. Biotechnol. Bioeng. **92:**147–159.
62. **Snoep, J. L., M. R. de Graef, A. H. Westphal, A. de Kok, M. J. Teixeira de Mattos, and O. M. Neijssel.** 1993. Differences in sensitivity to NADH of purified pyruvate dehydrogenase complexes of *Enterococcus faecalis*, *Lactococcus lactis*, *Azotobacter vinelandii*, and *Escherichia coli*: implications for their activity in vivo. FEMS Microbiol. Lett. **114:**279–283.
63. **Somsen, O. J. G., M. A. Hoeben, E. Esgalhado, J. L. Snoep, D. Visser, R. T. J. M. van der Heijden, J. J. Heijnen, and H. V. Westerhoff.** 2000. Glucose and the ATP paradox in yeast. Biochem. J. **352:**593–599.
64. **Stephanopoulos, G., A. A. Aristidou, and J. Nielsen.** 1998. Metabolic engineering: principles and methodologies. Academic Press, Inc., San Diego, CA.
65. **Stephanopoulos, G.** 1999. Metabolic fluxes and metabolic engineering. Metab. Eng. **1:**1–11.
66. **Szyperski, T.** 1995. Biosynthetically directed fractional ^{13}C-labeling of proteinogenic amino acids. An efficient analytical tool to investigate intermediary metabolism. Eur. J. Biochem. **232:**433–448.
67. **Underwood, S. A., S. Zhou, T. B. Causey, L. P. Yomano, K. T. Shanmugam, and L. O. Ingram.** 2002. Genetic changes to optimize carbon partitioning between ethanol and biosynthesis in ethanologenic *Escherichia coli*. Appl. Environ. Microbiol. **68:**6263–6272.
68. **van Winden, W. A., C. Wittman, E. Heinzle, and J. J. Heijnen.** 2002. Correcting mass isotopomer distributions for naturally occurring isotopes. Biotechnol. Bioeng. **80:**477–479.
69. **Veeger, C., D. V. DerVartanian, and W. P. Zeylemaker.** 1969. Succinate dehydrogenase. Methods Enzymol. **13:**81–90.
70. **Verduyn, C.** 1991. Physiology of yeasts in relation to biomass yield. Antonie van Leeuwenhoek **60:**325–353.
71. **Weitzman, P. D. J.** 1969. Citrate synthase from *Escherichia coli*. Methods Enzymol. **13:**22–26.
72. **Wiechert, W., and A. A. de Graaf.** 1997. Bidirectional reaction steps in metabolic networks: I. Modeling and simulation of carbon isotope labeling experiments. Biotechnol. Bioeng. **55:**101–117.
73. **Wiechert, W.** 2001. ^{13}C metabolic flux analysis. Metab. Eng. **3:**195–206.
74. **Yang, Y. T., K. Y. San, and G. N. Bennett.** 1999. Redistribution of metabolic fluxes in *Escherichia coli* with fermentative lactate dehydrogenase overexpression and deletion. Metab. Eng. **1:**141–152.
75. **Zhao, J., and K. Shimizu.** 2003. Metabolic flux analysis of *Escherichia coli* K12 grown on ^{13}C-labeled acetate and glucose using GC-MS and powerful flux calculation method. J. Biotechnol. **101:**101–117.
76. **Zhu, J., S. Shalel-Levanon, G. N. Bennett, and K. Y. San.** 2006. Effect of the global redox sensing/regulation networks on *Escherichia coli* and metabolic flux distribution based on C-13 labeling experiments. Metab. Eng. **8:**619–627.
77. **Zhu, J., S. Shalel-Levanon, G. N. Bennett, and K. Y. San.** 2007. The YfiD protein contributes to the pyruvate formate-lyase flux in an *Escherichia coli arcA* mutant strain. Biotechnol. Bioeng. **97:**138–143.
78. **Zupke, C., and G. Stephanopoulos.** 1994. Modeling of isotope distribution and intracellular fluxes in metabolic networks using atom mapping matrices. Biotechnol. Prog. **10:**489–498.